Rigorous transformation of variance–covariance matrices of GPS-derived coordinates and velocities

Tomás Soler · John Marshall

Abstract With the advances in the field of GPS positioning and the global densification of permanent GPS tracking stations, it is now possible to determine at the highest level of accuracy the transformation parameters connecting various international terrestrial reference frame (ITRF) realizations. As a by-product of these refinements, not only the seven usual parameters of the similarity transformations between frames are available, but also their rates, all given at some epoch t_k. This paper introduces rigorous matrix equations to estimate variance–covariance matrices for transformed coordinates at any epoch t based on a stochastic model that takes into consideration all a priori information of the parameters involved at epoch t_k, and the coordinates and velocities at the reference frame initial epoch t_0. The results of this investigation suggest that in order to attain maximum accuracy, the agencies determining the 14-parameter transformations between reference frames should also publish their full variance–covariance matrix.

Introduction

Fueled by the recent advancements of the global positioning system (GPS), our understanding about the behavior of geocentric terrestrial reference frames has substantially increased. The absolute accuracies currently available in geocentricity, orientation, and scale of terrestrial coordinate frames have surpassed anyone's prediction. The improvement is so significant that the variation with respect to time of the seven similarity transformation parameters can now be estimated. This achievement has been possible in part thanks to the refinements in post-fit precise ephemerides, which today provide the absolute orbital positions of the satellites at the ±5-cm level (Springer and Hugentobler 2001). As a result of this and other steady progressions (e.g., atmospheric delay models, precise antenna phase center offset calibrations, etc.), we have entered into a new, specialized realm of geodetic science that is purely geometrical in concept and strictly coordinate-based. Much effort has been dedicated to exploit this new bonanza of accurate positioning. For example, many countries have deployed permanent GPS tracking networks to provide accurate referencing by differential positioning techniques. In turn, their national geodetic control can now be easily densified at subcentimeter levels; a task unimaginable a decade ago. Furthermore, crustal motion and plate tectonic studies have become a routine practice, and deformations are now monitored continuously to detect displacements quickly and to track the increase of regional strain accumulation on a day-to-day basis. This scientific revolution in accurate positioning necessitates the full understanding of reference frames and their formal transformations. The fact that GPS terrestrial observing stations are located on moving lithospheric plates slightly complicates the issue, and the effects of such motions on the coordinates of the stations should be accurately taken into consideration. Similarly, individual velocities (absolute displacements) of the points in question should not be neglected and must be taken into account in any coordinate transformation where accurate results are expected.

Received: 1 June 2002 / Accepted: 10 July 2002
Published online: 12 October 2002

T. Soler (✉) · J. Marshall
National Geodetic Survey, NOS, NOAA, N/NGS22,
#8825, 1315 East–West Highway, Silver Spring,
MD 20910-3282, USA
E-mail: Tom.Soler@noaa.gov
Tel.: +1-301-7133205 ext. 157
Fax: +1-301-7134324

Notation

To facilitate the manipulation of mathematical expressions, a compact, flexible notation, particularly useful in three-dimensional transformations, will be advanced. Only right-handed, three-dimensional coordinate frames are used in this article. The following remarks are stressed about the notation introduced in this paper. By "notation" we mean a symbolic language able to translate concepts into mathematical equations regulated by matrix algebra operations. Matrix algebra is best suited to our purpose due to its simplicity, compactness, and directness. Because

 DOI 10.1007/s10291-002-0019-1

all discussions are restricted to three-dimensional Euclidean space, 3×1 three-dimensional column matrices will be abbreviated as follows: $\{x\}=\{x\ y\ z\}^t$, $\{T_x\}=\{T_x\ T_y\ T_z\}^t$, $\{v_x\}=\{v_x\ v_y\ v_z\}^t$, $\{v_e\}=\{v_e\ v_n\ v_u\}^t$, etc. The superscript t denotes, as usual, matrix transpose. Notice that the ordered sequence of coordinates is retained, although only the first coordinate appears explicitly as a subscript in the abbreviated notation. This direct notation is a short, compact way of representing vector matrices, and has the advantage of maintaining the matrix nomenclature popular in the solution of many problems that arise in different fields of engineering (e.g., finite element method) and particularly in aerospace and astronautical engineering.
The 3×3 identity (unit) matrix is denoted by $[I]$ and the zero (null) matrix of any dimension by $[0]$. For consistency, vectors will always be written between braces, matrices between brackets, and when applicable, scalars will be grouped between parentheses.
An abridged notation for 3×3 skew-symmetric (antisymmetric) matrices, so important when studying rotations, will be used throughout. To every arbitrary real vector $\{a\}=\{a_x\ a_y\ a_z\}^t$ it is possible to associate a skew-symmetric matrix denoted by:

$$\underline{[a]} = \begin{bmatrix} 0 & -a_z & a_y \\ a_z & 0 & -a_x \\ -a_y & a_x & 0 \end{bmatrix} \tag{1}$$

Some important well-known properties of skew-symmetric matrices are recalled:

$$\underline{[a]}^t = -\underline{[a]} \tag{2}$$

$$\underline{[a]}\{a\} = \{0\} \tag{3}$$

$$\underline{[a]}^2 = \{a\}\{a\}^t - (\{a\}^t\{a\})[I] \quad (\textit{symmetric matrix}) \tag{4}$$

$$\underline{[a]}^3 = -(\{a\}^t\{a\})\underline{[a]} \tag{5}$$

$$\underline{[a]}\{x\} = \underline{[x]}^t\{a\} \tag{6}$$

The advantage of the notation introduced here will be apparent when taking partials of matrix equations in Section 5.
If, in Eq. (1), the vector $\{a\}$ is replaced by the angular velocity vector $\{\Omega_x\}=\{\Omega_x\ \Omega_y\ \Omega_z\}^t$, the resulting skew-symmetric matrix represents a rotation operator that performs a body rotation where the points (i.e., position vectors) on the body rotate counterclockwise (anticlockwise), while the coordinate frame stays fixed. This rotation is consistent with a positive differential rotation of magnitude Ω about a single arbitrary axis (the Cartesian frame remains fixed). Figure 1 summarizes the two types of rotations encountered in practice in plate kinematics and in transformation of coordinate frames. All rotations are assumed anticlockwise positive and are based on the accepted definitions of elementary rotations of coordinate axes denoted by $R_i\ (\theta)$, i=1,2,3 (e.g., Kaula 1966, p. 13; Mueller 1969, p. 43) referred in the literature as "right-handed rotations". The three i subscripts indicate rotations about the first, second, and third axis, respectively. The argument represents the magnitude of the rotation, which, in most applications, is considered a small angle θ. The tacit convention in these formulas implies that the axes are rotated and points in space are held fixed; if the axes were fixed and the body of points rotated, the rotation matrices would have opposite signs [e.g., $R_i\ (-\theta)=R_i^t\ (\theta)$]. Successive rotations are operated in sequence; however,

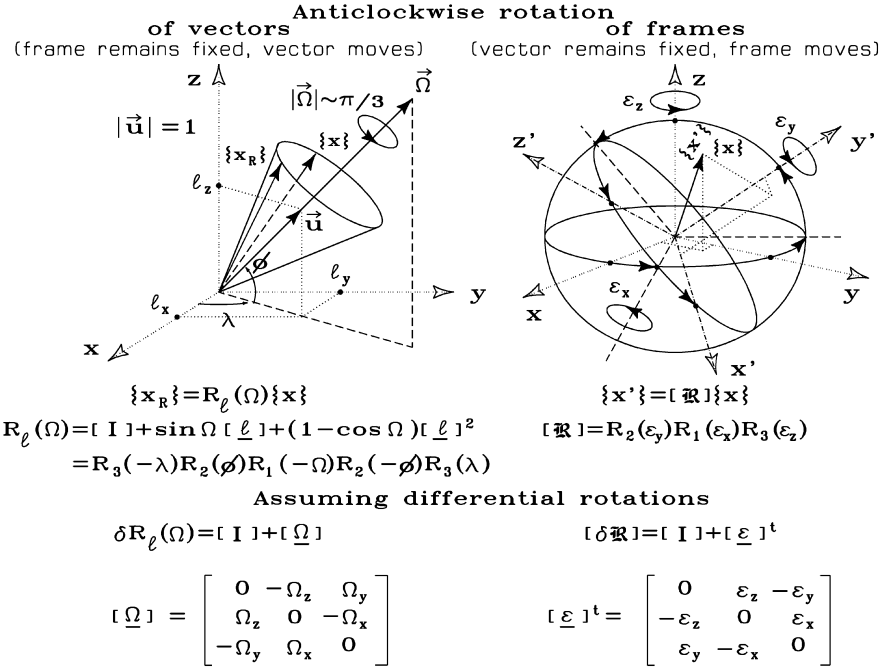

Fig. 1
Matrix transformations for anticlockwise rotations of vectors and frames

the final result is not commutative and depends on the specific sequence of the individual rotations applied. An exception to this rule is differential rotations, which follow the commutative property to first order.
The rotation sign convention adopted here is the one universally accepted when discussing rotations in mechanics and other areas of physics. It should be emphasized that a counterclockwise rotation of vectors is equivalent to a clockwise rotation of frames (the vector remains fixed in space). Consequently, when we want to rotate frame axes counterclockwise, as Fig. 1 shows, we should use the transpose of matrix (1). That is, if we want rotational consistency (all rotations positive when rotating on the same anticlockwise sense) one should use $[\Omega]$ for rotations of vectors around an arbitrary axis (e.g., plate kinematics) and $[\varepsilon]^t$ for differential rotations of magnitude ϵ_x, ϵ_y, and ϵ_z, respectively around the x, y, and z axes (frame rotations). Figure 1 summarizes all matrices involved in these two types of frequently used rotation operators. Recall that rotations of geocentric vectors about an arbitrary axis – while keeping the geocentric coordinate frame fixed– are required to properly account for plate tectonic motions. The above notation is consistent with the definition of fixed right-handed coordinate systems and positive anticlockwise rotation of vectors, which is labeled by some authors as the right-hand rule. This sign convention is the one primarily used in rigid body mechanics and widely adopted by geophysicists investigating plate kinematics.

Geocentric terrestrial (Earth-fixed) conventional reference frames

With the advent of GPS, the possibility of directly measuring three-dimensional Cartesian coordinates to the subcentimeter level has drastically changed the methodology used in geodesy, surveying, and mapping applications. The discussions that follow are restricted to the family of international terrestrial reference frames (ITRF). They are consistently assessed as the most rigorously defined set of geocentric terrestrial frames and the only ones providing the variation with respect to time of the similarity transformation parameters and their standard errors.
As of this writing (September 2002), ITRF00 is the latest realization (based on data including up to epoch 2000.0) of a series of ITRF geocentric conventional terrestrial reference frames determined by the International Earth Rotation Service (IERS) headquartered in Paris, France. The ITRF solutions incorporate extraterrestrial data from several sources (VLBI, SLR, GPS, and DORIS (Doppler Orbitography and Radiopositioning Integrated by Satellite)). ITRF frames are created under international sponsorship and satisfy stringent criteria required by modern space systems. Related to each ITRF frame there is an associated velocity field, i.e., each point of the network materializing the frame has affixed a velocity vector with three components (v_x, v_y, v_z) indicating its time-dependent absolute displacements caused, primarily, by the motion of the tectonic plate on which the point is located. Coordinates and velocities referred to some particular ITRF frame are always given at some initial epoch t_0. This precaution is required to take into account the motion of the observing stations, which is inevitable due to the phenomena of plate tectonics. Nevertheless, plate rotations can be approximated anywhere on the Earth's crust by spherical geophysical models such as NNR-NUVEL1A (DeMets et al. 1994), which is a revised improvement of the original NUVEL-1 (Argus and Gordon 1991).

Transformations between geocentric conventional terrestrial frames

When transforming coordinates between geocentric conventional terrestrial frames of the ITRF type, one should also keep in mind that all parameters involved in the transformation are given at some specific epoch t_k, and that, in general, $t_k \neq t_0$. Coordinates referred to the ITRFyy, epoch t_0 (yy denotes the last two digits of the ITRF yearly solution, e.g., ITRF00), family of frames have attached, as explained above, a velocity field giving at every point the corresponding components of the linear velocity (v_x, v_y, v_z) and their standard errors $\sigma_{v_x}, \sigma_{v_y}, \sigma_{v_z}$ about the three local terrestrial Cartesian axes.
Many of the GPS ITRF sites are sponsored by the International GPS Service (IGS), which maintains a selected global network of receivers continuously tracking satellites of the GPS constellation (Moore 2002). The location of these IGS receivers, as well as, e.g., the National Geodetic Survey (NGS) Continuously Operating Reference Stations (National CORS) network (Snay and Weston 1999), are useful as "fiducial" stations to propagate coordinates in global/regional GPS surveys. The term "fiducial" is loosely applied here to describe continuously operating GPS sites whose RINEX2 data are made available electronically, free of charge, to the geodetic-surveying community. The coordinates and velocities of these permanent sites are accurately known with respect to ITRF00 and could be used to rigorously propagate coordinates to other arbitrary points. Establishing permanent GPS networks has been one of the major breakthroughs for geodesy and precise surveying in the last decade.

Theoretical considerations

The most general transformation between two frames could be represented symbolically by the mapping $ITRF_{yy}(t_0) \rightarrow ITRF_{zz}(t)$ established through 14 transformation parameters. The foundation of the 14-parameter transformation rests in the well-known seven-parameter similarity transformation

$$\{x(t_0)\}_{ITRFzz} = \{T_x\} + \sigma[\Re]\{x(t_0)\}_{ITRFyy} \quad (7)$$

where $\{T_x\}$ denotes the translation or shifts between the two frames, σ is the scale and $[\Re]$ is the frame rotation matrix. Further, the 14-parameter transformation also

relies on the following expressions that relate a position at times t and t_0 through a velocity v

$$\{x(t)\}_{ITRFzz} = \{x(t_0)\}_{ITRFzz} + (t - t_0)\{v_x(t_0)\}_{ITRFzz} \quad (8)$$

$$\{x(t)\}_{ITRFyy} = \{x(t_0)\}_{ITRFyy} + (t - t_0)\{v_x(t_0)\}_{ITRFyy} \quad (9)$$

Additionally, the seven time-dependent parameters in the 14-parameter transformation arise by taking the derivative of Eq. (7) with respect to time, illustrated as

$$\begin{aligned}\{\dot{x}(t_0)\}_{ITRFzz} \equiv \{v_x(t_0)\}_{ITRFzz} = \{\dot{T}_x\} + \dot{\sigma}[\Re]\{x(t_0)\}_{ITRFyy} \\ + \sigma[\dot{\Re}]\{x(t_0)\}_{ITRFyy} \\ + \sigma[\Re]\{v_x(t_0)\}_{ITRFyy}\end{aligned} \quad (10)$$

The complete expression containing 14 parameters is obtained by substituting Eqs. (7) and (10) into Eq. (8) and assuming differential values for the 14 parameters. The general expression is a generalization of the formulation previously given in (Soler 1998) and in explicit form could be written

In the above equations t_k is the epoch at which the transformation parameters are given, t_0 is the epoch of the initial frame, and t the epoch of the final transformed frame. The vector $\{T_x(t_k)\}$ contains the coordinates of the origin of the frame *ITRFyy* in the frame *ITRFzz*, i.e., the translations or shifts between the two frames; $\varepsilon_x(t_k), \varepsilon_y(t_k), \varepsilon_z(t_k)$ are differential counterclockwise (anticlockwise) rotations (expressed in radians ≡ rad), respectively, around the axes x, y, and z of the *ITRFyy* frame to establish parallelism with the *ITRFzz* frame, and s is the differential scale change (expressed in ppm $\times 10^{-6}$; ppm = parts per million). The coordinates $\{x\}$ and the velocities $\{v_x\}$ must have conformable units, usually meters and m/year (≡ m/y), respectively. The time intervals t_k–t_0 and t–t_k are generally expressed in year and its fraction. Note that t could be the actual time of the GPS observations (e.g., t =2003.5783). Sometimes, in order to compare results with previous geodynamic studies, one could be interested in the inverse transformation: $ITRF_{zz}(t) \rightarrow ITRF_{yy}(t_0)$. Table 1 gives the most recently determined transformation parameters and their rates between the IGS realizations of *ITRF*97 and *ITRF*00 at epoch 01 July 2001 (Ferland 2002).

$$\begin{aligned}\begin{Bmatrix} x(t) \\ y(t) \\ z(t) \end{Bmatrix}_{ITRFzz} &= \begin{Bmatrix} T_x(t_k) \\ T_y(t_k) \\ T_z(t_k) \end{Bmatrix} + (1 + s(t_k)) \begin{bmatrix} 1 & \varepsilon_z(t_k) & -\varepsilon_y(t_k) \\ -\varepsilon_z(t_k) & 1 & \varepsilon_x(t_k) \\ \varepsilon_y(t_k) & -\varepsilon_x(t_k) & 1 \end{bmatrix} \begin{Bmatrix} x(t_k) \\ y(t_k) \\ z(t_k) \end{Bmatrix}_{ITRFyy} \\ &+ (t - t_k)\left[\left[\begin{Bmatrix} \dot{T}_x \\ \dot{T}_y \\ \dot{T}_z \end{Bmatrix} + \left[(1 + s(t_k)) \begin{bmatrix} 0 & \dot{\varepsilon}_z & -\dot{\varepsilon}_y \\ -\dot{\varepsilon}_z & 0 & \dot{\varepsilon}_x \\ \dot{\varepsilon}_y & -\dot{\varepsilon}_x & 0 \end{bmatrix} + \dot{s} \begin{bmatrix} 1 & \varepsilon_z(t_k) & -\varepsilon_y(t_k) \\ -\varepsilon_z(t_k) & 1 & \varepsilon_x(t_k) \\ \varepsilon_y(t_k) & -\varepsilon_x(t_k) & 1 \end{bmatrix}\right] \begin{Bmatrix} x(t_k) \\ y(t_k) \\ z(t_k) \end{Bmatrix}_{ITRFyy}\right]\right] \\ &+ (t - t_k)\left[\left[(1 + s(t_k)) \begin{bmatrix} 1 & \varepsilon_z(t_k) & -\varepsilon_y(t_k) \\ -\varepsilon_z(t_k) & 1 & \varepsilon_x(t_k) \\ \varepsilon_y(t_k) & -\varepsilon_x(t_k) & 1 \end{bmatrix} \begin{Bmatrix} v_x(t_k) \\ v_y(t_k) \\ v_z(t_k) \end{Bmatrix}_{ITRFyy}\right]\right]\end{aligned} \quad (11)$$

where:

$$\begin{Bmatrix} x(t_k) \\ y(t_k) \\ z(t_k) \end{Bmatrix}_{ITRFyy} = \begin{Bmatrix} x(t_0) \\ y(t_0) \\ z(t_0) \end{Bmatrix}_{ITRFyy} + (t_k - t_0) \begin{Bmatrix} v_x(t_0) \\ v_y(t_0) \\ v_z(t_0) \end{Bmatrix}_{ITRFyy} \quad (12)$$

Assuming that, without loss of generality, on the same frame $\{v_x(t_k)\} \approx \{v_x(t_0)\}$, we have after combining the second and last terms of Eq. (11) and making use of Eq. (12):
Switching to the compact matrix notation explained in Section 2, we can write the above equation as:

Table 1
Most recent 14-transformation parameters between modern geocentric frames (Ferland 2002, p. 26). IGS(ITRF2000) → IGS(ITRF97) (epoch: t_k=2001.5). *mas* Milliarc second; *ppb* parts per billion =10^{-3} ppm. Anticlockwise rotations of amounts ϵ_x, ϵ_y, ϵ_z about the x, y, and z axes are assumed positive

T_x (m)	T_y (m)	T_z (m)	ϵ_x (mas)	ϵ_y (mas)	ϵ_z (mas)	s (ppb)
0.0047	0.0028	–0.0256	–0.030	–0.003	–0.140	1.48
±0.0005	±0.0006	±0.0008	±0.025	±0.021	±0.021	±0.09
$\dot{T}_x$(m/y)	$\dot{T}_y$(m/y)	$\dot{T}_z$(m/y)	$\dot{\varepsilon}_x$(mas/y)	$\dot{\varepsilon}_y$(mas/y)	$\dot{\varepsilon}_z$(mas/y)	$\dot{s}$(ppb/y)
–0.0004	–0.0008	–0.0016	0.003	–0.001	–0.030	0.03
±0.0003	±0.0003	±0.0004	±0.012	±0.011	±0.011	±0.05

$$\begin{Bmatrix} x(t) \\ y(t) \\ z(t) \end{Bmatrix}_{ITRFzz} = \begin{Bmatrix} T_x(t_k) \\ T_y(t_k) \\ T_z(t_k) \end{Bmatrix} + (1+s(t_k)) \begin{bmatrix} 1 & \varepsilon_z(t_k) & -\varepsilon_y(t_k) \\ -\varepsilon_z(t_k) & 1 & \varepsilon_x(t_k) \\ \varepsilon_y(t_k) & -\varepsilon_x(t_k) & 1 \end{bmatrix} \left[\begin{Bmatrix} x(t_0) \\ y(t_0) \\ z(t_0) \end{Bmatrix} + (t-t_0) \begin{Bmatrix} v_x(t_0) \\ v_y(t_0) \\ v_z(t_0) \end{Bmatrix} \right]_{ITRFyy}$$
$$+(t-t_k) \left[\left[\begin{Bmatrix} \dot{T}_x \\ \dot{T}_y \\ \dot{T}_z \end{Bmatrix} + \left[(1+s(t_k)) \begin{bmatrix} 0 & \dot{\varepsilon}_z & -\dot{\varepsilon}_y \\ -\dot{\varepsilon}_z & 0 & \dot{\varepsilon}_x \\ \dot{\varepsilon}_y & -\dot{\varepsilon}_x & 0 \end{bmatrix} + \dot{s} \begin{bmatrix} 1 & \varepsilon_z(t_k) & -\varepsilon_y(t_k) \\ -\varepsilon_z(t_k) & 1 & \varepsilon_x(t_k) \\ \varepsilon_y(t_k) & -\varepsilon_x(t_k) & 1 \end{bmatrix} \right] \begin{Bmatrix} x(t_k) \\ y(t_k) \\ z(t_k) \end{Bmatrix}_{ITRFyy} \right] \right] \quad (13)$$

$$\{x(t)\}_{ITRFzz} = \{T_x\} + (1+s)[\delta\Re][\{x(t_0)\}_{ITRFyy} + (t-t_0)\{v_x(t_0)\}_{ITRFyy}] + (t-t_k)[[\{\dot{T}_x\} + [(1+s)\underline{[\dot{\varepsilon}]}^t + \dot{s}\,[\delta\Re]]\{x(t_k)\}_{ITRFyy}]] \quad (14)$$

where the matrix symbols used could be easily identified by direct one-to-one comparison with its explicit form given by Eq. (13). Notice that $[\delta\Re] = [I] + \underline{[\varepsilon]}^t$ represents the differential rotation matrix between the two frames. Finally, as a function of the coordinates at time t_0, we have;

$$\{x(t)\}_{ITRFzz} = \{T_x\} + (1+s)[\delta\Re][\{x(t_0)\}_{ITRFyy} + (t-t_0)\{v_x(t_0)\}_{ITRFyy}] + (t-t_k)[[\{\dot{T}_x\} + [(1+s)\underline{[\dot{\varepsilon}]}^t + \dot{s}\,[\delta\Re]]\{\{x(t_0)\}_{ITRFyy} + (t_k-t_0)\{v_x(t_0)_{ITRFyy}\}\}] \quad (15)$$

If we further assume t_k=t_0, we arrive at the equations given in (Soler 1998), namely,

$$\{x(t)\}_{ITRFzz} = \{T_x\} + (1+s)[\delta\Re][\{x(t_0)\}_{ITRFyy} + (t-t_0)\{v_x(t_0)\}_{ITRFyy}] + (t-t_0)[[\{\dot{T}_x\} + [(1+s)\underline{[\dot{\varepsilon}]}^t + \dot{s}\,[\delta\Re]]\{x(t_0)\}_{ITRFyy}]] \quad (16)$$

Summarizing, the following transformations between frames are possible:

$ITRF_{yy}(t_0) \rightarrow ITRF_{zz}(t)\ ;\ \ t \neq t_k \neq t_0$ *Required* { 14 *parameters at epoch* t_k ; *Coordinates & velocities in* $ITRF_{yy}$ *at epoch* t_0 }

$ITRF_{yy}(t_0) \rightarrow ITRF_{zz}(t)\ ;\ \ t \neq t_k = t_0$ *Required* { 14 *parameters at epoch* t_0 ; *Coordinates & velocities in* $ITRF_{yy}$ *at epoch* t_0 }

$ITRF_{yy}(t_0) \rightarrow ITRF_{zz}(t_0)\ ;\ \ t = t_0 \neq t_k$ *Required* { 14 *parameters at epoch* t_k ; *Coordinates & velocities in* $ITRF_{yy}$ *at epoch* t_0 }

$ITRF_{yy}(t_0) \rightarrow ITRF_{zz}(t)\ ;\ \ t \neq t_k = t_0$ *and* $\{v_x(t_0)\} = \{0\}$; *Datum problem* { $14 -$ *parameters at epoch* t_0 ; *Coordinates in* $ITRF_{yy}$ *at epoch* t_0 }

$ITRF_{yy}(t_0) \rightarrow ITRF_{zz}(t)\ ;\ \ t = t_k \neq t_0$ *Required* { 7 *parameters at epoch* t_0 ; *Coordinates & velocities in* $ITRF_{yy}$ *at epoch* t_0 }

$ITRF_{yy}(t_0) \rightarrow ITRF_{zz}(t_0)\ ;\ \ t = t_k = t_0$ *Required* { 7 *parameters at epoch* t_0 (*Helmert's Transformation*) ; *Coordinates in* $ITRF_{yy}$ *at epoch* t_0 }

$ITRF_{yy}(t_0) \rightarrow ITRF_{yy}(t)\ ;$ *Required* : *velocities of* $ITRF_{yy}$ *at* t_0

$ITRF_{yy}(t_0) \rightarrow ITRF_{yy}(t_0)$; *identity* : *Transformation parameters & velocities* $= 0$

The formulation to rigorously transform velocities between two epochs t_0 and t, and $t_k \neq t_0$ could be obtained by taking partials with respect to time t in Eq. (15). The resulting final expression is:

$$\{v_x(t)\}_{ITRFzz} = \{\dot{T}_x\} + [[(1+s)\,\underline{[\dot{\varepsilon}]}^t + \dot{s}\,[\delta\Re]]x(t_0)\}_{ITRFyy} + [[(1+s)[\delta\Re] + (t_k-t_0)\,[(1+s)\,\underline{[\dot{\varepsilon}]}^t + \dot{s}\,[\delta\Re]]]\,\{v_x(t_0)\}_{ITRFyy} \quad (17)$$

In the particular case that t_k=t_0, after substituting $\{x\} \equiv \{x(t_0)\}$, $\{v_x\} \equiv \{v_x(t_0)\}$, and neglecting

second order terms, the equation above reduces to the equation already given in (Soler 1998), namely

$$\{v_x\}_{ITRFzz} = \{\dot{T}_x\} + [\![(1+s)\,\underline{[\dot{\varepsilon}]}^t + \dot{s}\,[\delta\Re]]\!]\{x\}_{ITRFyy} + (1+s)[\delta\Re]\,\{v_x\}_{ITRFyy} \quad (18)$$

Note that Eqs. (11) and (17) are more general than the ones in (Soler 1998) and others that subsequently appeared in the literature (e.g., Boucher et al. 1999). In this particular reference, although not mentioned in the text, the authors neglect higher than second-order contributions and thus assume the following simplifications: $s\,\underline{[\varepsilon]}^t = s\,\underline{[\dot{\varepsilon}]}^t = \dot{s}\,\underline{[\varepsilon]}^t = [0]$, and $\underline{[\varepsilon]}^t\{v_x\} = s\{v_x\} = \{0\}$. None of these works include the mathematical extension to the determination of variance–covariance matrices, which is discussed later in this paper.

Sometimes, the value of the station velocity vector $\{v_x\}$ is not readily known. This is clearly the situation for GPS stations that do not belong to the set of CORS or IGS global sites. Then, approximations could be obtained by using any of the published kinematic plate models. In such case, the angular velocity components $\{\Omega_x\}_{Pi}$ for each plate P_i, are known quantities that could be extracted from the available geophysical models. Accordingly, the velocity vector $\{v_x\}$ required in Eqs. (11), (12), and (17) could be approximated as follows

$$\{v_x\}_{ITRFyy} \approx \underline{[\Omega]}_{P_i}\{x\}_{ITRFyy} = \begin{bmatrix} 0 & -\Omega_z & \Omega_y \\ \Omega_z & 0 & -\Omega_x \\ -\Omega_y & \Omega_x & 0 \end{bmatrix}_{P_i} \begin{Bmatrix} x \\ y \\ z \end{Bmatrix}_{ITRFyy} \quad (19)$$

Here, $\{v_x\}$ represents the three components of velocity (along the x, y, and z ITRF local axes) of a point, whose position vector is $\{x\}$, due to an infinitesimal rotation of amount Ω about an axis through the origin directed along the rotation pole of the plate. The elements of $\underline{[\Omega]}_{P_i}$ have units of rad/y and contain angular velocity components $\{\Omega_x\}_{Pi}$ of the particular plate P_i on which the point is located. These components are given in, e.g., McCarthy (1996, p. 14) for the model (no net rotation) NNR-NUVEL1A in rad/My (My ≡ million years). They are also tabulated in Table 2, transformed to units of milliarc second/year (≡ mas/y), which are quantities easier to visualize. The spherical longitude (λ) and latitude (ϕ) of the axis along the vector $\vec{\Omega}$ defining the rotation pole is straightforward from the equations:

$$\lambda = \arctan\frac{\Omega_y}{\Omega_x};\quad 0 \le \lambda \le 2\pi \quad (20)$$

$$\phi = \arctan\frac{\Omega_z}{\sqrt{\Omega_x^2 + \Omega_y^2}};\quad -\frac{\pi}{2} \le \phi \le \frac{\pi}{2} \quad (21)$$

At a minimum, station velocities should be applied to the fiducial sites before starting GPS processing in order to bring the position of these reference stations as close as possible to their actual spatial location at the time the observations were collected. For consistency, the selected reference frame for all fiducial points should be the one implicit in the precise ephemeris used during processing, consequently the resulting coordinates are referred to the reference frame of the satellite orbits used and the actual epoch of observation. The final processed GPS coordinates could be rigorously transformed to any other conventional terrestrial frame using Eqs. (11) and (12) and a set of parameters such as the ones tabulated in Table 1.

If preferred, for better practical visualization, the velocity components could be expressed along the local east-north-up frame (e, n, u):

$$\{v_e\} = [\mathrm{R}]\{v_x\}. \quad (22)$$

where [R] is the well-known rotation (proper orthogonal) matrix of the transformation between local geocentric and local geodetic frames which can be conveniently expressed as:

$$[\mathrm{R}] = \mathrm{R}_1(\pi/2 - \varphi)\mathrm{R}_3(\lambda + \pi/2) = \mathrm{R}_3(\pi/2)\mathrm{R}_2(\pi/2 - \varphi)\mathrm{R}_3(\lambda) \quad (23)$$

where the curvilinear coordinates λ and φ denote geodetic longitude and latitude, respectively.

Table 2
Cartesian rotation vector for each major plate using the NNR-NUVEL1A kinematic plate model (no net rotation). *mas* Milliarc second. Anticlockwise rotations of magnitude $\left|\vec{\Omega}\right|$ around each plate polar axis (defined by the vector $\vec{\Omega}$) are assumed positive

Plate name	Ω_x (mas/y)	Ω_y (mas/y)	Ω_z (mas/y)	$\left\|\vec{\Omega}\right\|$ (mas/y)
Africa	0.1837	–0.6392	0.8090	1.047283
Antarctica	–0.1693	–0.3508	0.7644	0.857922
Arabia	1.3789	–0.1075	1.3943	1.963923
Australia	1.6169	1.0569	1.2957	2.325992
Caribbean	–0.0367	–0.6982	0.3261	0.771473
Cocos	–2.1503	–4.4563	2.2534	5.436930
Eurasia	–0.2023	–0.4940	0.6503	0.841339
India	1.3758	0.0082	1.4005	1.407265
Nazca	–0.3160	–1.7691	1.9820	2.675424
North America	0.0532	–0.7423	–0.0316	0.744874
Pacific	–0.3115	0.9983	–2.0564	2.307036
South America	–0.2141	–0.3125	–0.1794	0.419141
Philippines	2.0812	–1.4768	–1.9946	3.238944

Variance–covariance matrix of transformed coordinates and velocities

The main intent of this investigation is to introduce a rigorous formalism for transforming variance–covariance matrices of coordinates and velocities from epoch t_0 to epoch t as a function of the initial variance–covariance matrix of the coordinates and velocities referred to ITRFyy at t_0 and the variance–covariance matrices of the fourteen-parameters connecting the two frames at epoch t_k. In brief, and for readers familiar with IGS nomenclature, the intent

is to transform between SINEX (software independent exchange format) files and epochs.
Mathematically, according to "error propagation law", we can write:

$$\Sigma_{S'} = [J]\ \Sigma_S\ [J]^t \tag{24}$$

where the a priori known symmetric variance–covariance matrix Σ_s is of the form:

$$\Sigma_S = \begin{bmatrix} \Sigma_C & \Sigma_{CV} & \Sigma_{CP} & \Sigma_{C\dot{P}} \\ \Sigma_{VC} & \Sigma_V & \Sigma_{VP} & \Sigma_{V\dot{P}} \\ \Sigma_{PC} & \Sigma_{PV} & \Sigma_P & \Sigma_{P\dot{P}} \\ \Sigma_{\dot{P}C} & \Sigma_{\dot{P}V} & \Sigma_{\dot{P}P} & \Sigma_{\dot{P}} \end{bmatrix} \tag{25}$$

and the meaning of the subindices are C coordinates, V velocities, P transformation parameters, and $\dot{P}$ rate-of-change of P. For clarity, the explicit form of the symmetric matrix Σ_C is given below:

$$\Sigma_C = \begin{bmatrix} \Sigma_{x_1} & \Sigma_{x_1x_2} & \cdots & \Sigma_{x_1x_n} \\ \Sigma_{x_2x_1} & \Sigma_{x_2} & \cdots & \Sigma_{x_2x_n} \\ \vdots & \vdots & \ddots & \vdots \\ \Sigma_{x_nx_1} & \Sigma_{x_nx_2} & \cdots & \Sigma_{x_n} \end{bmatrix}_{(3n\times 3n)} \quad (symmetric) \tag{26}$$

and $\forall i$=1,...,n; j=1,...,n (n = total number of points) the diagonal blocks and the positions cross-covariances will be (3×3) matrices of the form:

$$\Sigma_{x_i} = \begin{bmatrix} \sigma_x^2 & \sigma_{xy} & \sigma_{xz} \\ \sigma_{yx} & \sigma_y^2 & \sigma_{yz} \\ \sigma_{zx} & \sigma_{zy} & \sigma_z^2 \end{bmatrix}_i (symmetric); \qquad \Sigma_{x_ix_j} = \begin{bmatrix} \sigma_{x_ix_j} & \sigma_{x_iy_j} & \sigma_{x_iz_j} \\ \sigma_{y_ix_j} & \sigma_{y_iy_j} & \sigma_{y_iz_j} \\ \sigma_{z_ix_j} & \sigma_{z_iy_j} & \sigma_{z_iz_j} \end{bmatrix} (non\ symmetric) \tag{27}$$

where obviously $\Sigma_{x_jx_i} = \Sigma^t_{x_ix_j}$. Although not given here explicitly, the same logic applies to the matrix Σ_V which is also $3n$×$3n$ and can be written from (26) after replacing the subindex x by v_x. The above arguments could be extended to the cross-covariance matrix Σ_{CV}, which also fulfills the property Σ_{VC}=Σ^t_{CV}.
The variance–covariance matrix of the transformation parameters can be written as:

$$\Sigma_P = \begin{bmatrix} \Sigma_T & \Sigma_{T[\varepsilon s]} \\ \Sigma_{[\varepsilon s]T} & \Sigma_{[\varepsilon s]} \end{bmatrix} \tag{28}$$

where Σ_T is the 3×3 variance–covariance matrix of the origin shifts and

$$\Sigma_{[\varepsilon s]} = \begin{bmatrix} \sigma^2_{\varepsilon_x} & \sigma_{\varepsilon_x\varepsilon_y} & \sigma_{\varepsilon_x\varepsilon_z} & \sigma_{\varepsilon_x s} \\ \sigma_{\varepsilon_y\varepsilon_x} & \sigma^2_{\varepsilon_y} & \sigma_{\varepsilon_y\varepsilon_z} & \sigma_{\varepsilon_y s} \\ \sigma_{\varepsilon_z\varepsilon_x} & \sigma_{\varepsilon_z\varepsilon_y} & \sigma^2_{\varepsilon_z} & \sigma_{\varepsilon_z s} \\ \sigma_{s\varepsilon_x} & \sigma_{s\varepsilon_y} & \sigma_{s\varepsilon_z} & \sigma^2_s \end{bmatrix}_{(4\times 4)} \quad (symmetric) \tag{29}$$

An equation similar to (28) can be written for $\Sigma\dot{P}$.
In the majority of practical cases, some of the cross-covariances in Eq. (25) are not known and assumed to be zero, thus, independent of matrix dimensions we may write:

$$\Sigma_{CP} = \Sigma_{C\dot{P}} = \Sigma_{VP} = \Sigma_{V\dot{P}} = \Sigma_{P\dot{P}} = [0] \tag{30}$$

Furthermore, the block matrices Σ_P and $\Sigma_{\dot{P}}$ are, generally speaking, full matrices with corresponding cross-covariance matrix $\Sigma_{P\dot{P}}$. However, for unknown reasons, the agencies disseminating the values of the 14 transformation parameters only publish the diagonal elements of Σ_P and $\Sigma_{\dot{P}}$. To benefit variance-covariance analyses, all elements of matrices Σ_P, $\Sigma_{\dot{P}}$, and $\Sigma_{P\dot{P}}$ should be disseminated; this will be the only way to know the full impact of assuming the non-diagonal elements to be zero.
The Jacobian matrix $[J]$ of Eq. (24) involves two mathematical models, one related to the positions and the other to the velocities, basically, Eqs. (15) and (17).
Equation (15) may be expressed as the compact functional relationship:

$$C' = \Im(C,\ V,\ P,\ \dot{P}) \tag{31}$$

Similarly, Eq. (17) takes the form:

$$V' = \mathcal{A}(C,\ V,\ P,\ \dot{P}) \tag{32}$$

Consequently, the Jacobian $[J]$ is composed of the following submatrices:

$$[J] = \begin{bmatrix} [\partial\Im/\partial C]_{(3n\times 3n)} & [\partial\Im/\partial V]_{(3n\times 3n)} & [\partial\Im/\partial P]_{(3n\times 7)} & [\partial\Im/\partial\dot{P}]_{(3n\times 7)} \\ [\partial\mathcal{A}/\partial C]_{(3n\times 3n)} & [\partial\mathcal{A}/\partial V]_{(3n\times 3n)} & [\partial\mathcal{A}/\partial P]_{(3n\times 7)} & [\partial\mathcal{A}/\partial\dot{P}]_{(3n\times 7)} \end{bmatrix}_{(6n)\times(6n+14)} \tag{33}$$

Contribution of Eq. (15) to the Jacobian

Representing explicitly Eq. (15) as the following functional relationship:

$$X = \Im(Y) = \Im\left(x_i, y_i, z_i, v_{xi}, v_{yi}, v_{zi}, T_x, T_y, T_z, \varepsilon_x, \varepsilon_y, \varepsilon_z, s, \dot{T}_x, \dot{T}_y, \dot{T}_x, \dot{\varepsilon}_x, \dot{\varepsilon}_y, \dot{\varepsilon}_z, \dot{s}\right) \tag{34}$$

i=1,..., n (n = total number of points in the transformation).

The partial derivatives of matrix Eq. (15) must be determined to obtain the Jacobian matrix $[J]$ required in

Eq. (24). To facilitate this computation the following symbolic vector differentiation definitions will be introduced:

$$\partial(\{x\})/\partial\{x\} = [I] \tag{35}$$

For any arbitrary 3×3 scalar matrix $[A]$:

$$\partial([A]\{x\})/\partial\{x\} = [A] \tag{36}$$

Notice that some of the final matrices presented above are dependent on the coordinates and velocities of each point, thus one will have to compute them at each point i: $[\partial\varepsilon]_i, \{\partial s\}_i, [\partial\dot{\varepsilon}]_i, \{\partial\dot{s}\}_i$, $i = 1,...,n$ replacing, when appropriate, the corresponding vectors $\{x\}_i$ and/or $\{v_x\}_i$. Thus, the final elements (submatrices) of the contribution to the Jacobian matrix $[J]$ can be written in compact form as

$$[C] = \begin{bmatrix} [\partial x] & [0] & \dots & [0] & | & [\partial v] & [0] & \dots & [0] \\ [0] & [\partial x] & \dots & [0] & | & [0] & [\partial v] & \dots & [0] \\ \vdots & \vdots & & \vdots & | & \vdots & \vdots & & \vdots \\ [0] & [0] & \dots & [\partial x] & | & [0] & [0] & \dots & [\partial v] \end{bmatrix}_{(3n\times 6n)} = \underset{3n\times 3n}{[\,[C_1]} \vdots \underset{3n\times 3n}{[C_2]\,]} \tag{46}$$

and

$$[D] = \begin{bmatrix} [I] & | & [\partial\varepsilon]_1 & | & \{\partial s\}_1 & | & (t-t_k)[I] & | & [\partial\dot{\varepsilon}]_1 & | & \{\partial\dot{s}\}_1 \\ [I] & | & [\partial\varepsilon]_2 & | & \{\partial s\}_2 & | & (t-t_k)[I] & | & [\partial\dot{\varepsilon}]_2 & | & \{\partial\dot{s}\}_2 \\ \vdots & | & \vdots & | & \vdots & | & \vdots & | & \vdots & | & \vdots \\ [I] & | & [\partial\varepsilon]_n & | & \{\partial s\}_n & | & (t-t_k)[I] & | & [\partial\dot{\varepsilon}]_n & | & \{\partial\dot{s}\}_n \end{bmatrix}_{(3n\times 14)} = \underset{3n\times 7}{[[D_1]} \vdots \underset{3n\times 7}{[D_2]]} \tag{47}$$

and finally,

$$\partial\left(\underline{[\varepsilon]}^t\{x\}\right)/\partial\{\varepsilon\} = \underline{[x]} \tag{37}$$

In the following derivations and to simplify notation, the identities $\{x(t_0)\} \equiv \{x\}$, and $\{v_x(t_0)\} \equiv \{v_x\}$ are introduced. Taking partial derivatives of Eq. (15) with respect to the parameters, after using the above definitions we obtain:

$$\partial\Im/\partial\{x\} = (1+s)[\delta\Re] + (t-t_k)\,[[(1+s)\underline{[\dot{\varepsilon}]}^t + \dot{s}\,[\delta\Re]\,]] = [\partial x] \tag{38}$$

$$\partial\Im/\partial\{v_x\} = (t-t_0)(1+s)[\delta\Re] + (t-t_k)(t_k-t_0) \times \left[\left[(1+s)\underline{[\dot{\varepsilon}]}^t + \dot{s}\,[\delta\Re]\right]\right] = [\partial v_x] \tag{39}$$

$$\partial\Im/\partial\{T_x\} = [I] \tag{40}$$

$$\partial\Im/\partial\{\varepsilon\} = (1+s)[[\underline{[x]} + (t-t_0)\,\underline{[v_x]}\,]] + (t-t_k)\,\dot{s}\,[[\underline{[x]} + (t_k-t_0)\underline{[v_x]}]] = [\partial\varepsilon] \tag{41}$$

$$\partial\Im/\partial s = [\delta\Re][\{x\} + (t-t_0)\{v_x\}] + (t-t_k)\,\underline{[\dot{\varepsilon}]}^t[[\{x\} + (t_k-t_0)\{v_x\}]] = \{\partial s\} \tag{42}$$

$$\partial\Im/\partial\{\dot{T}_x\} = (t-t_k)\,[I] \tag{43}$$

$$\partial\Im/\partial\{\dot{\varepsilon}\} = (t-t_k)(1+s)[[\,\underline{[x]} + (t_k-t_0)\underline{[v_x]}\,]] = [\partial\dot{\varepsilon}] \tag{44}$$

$$\partial\Im/\partial\dot{s} = (t-t_k)[\delta\Re]\,[[\{x\} + (t_k-t_0)\{v_x\}]] = \{\partial\dot{s}\} \tag{45}$$

Contribution of Eq. (17) to the Jacobian

Following a procedure similar to the one described above, the partial derivatives of the function

$$V' = \mathcal{A}(Z) = \mathcal{A}(x_i, y_i, z_i, v_{x_i}, v_{y_i}, v_{z_i}, \varepsilon_x, \varepsilon_y, \varepsilon_z, s, \dot{T}_x, \dot{T}_y, \dot{T}_z, \dot{\varepsilon}_x, \dot{\varepsilon}_y, \dot{\varepsilon}_z, \dot{s}) \tag{48}$$

could be determined as follows:

$$\partial\mathcal{A}/\partial\{x\} = \partial[\partial x]/\partial t = (1+s)\underline{[\dot{\varepsilon}]}^t + \dot{s}[\delta\Re] = \left[\bar{\partial}x\right] \tag{49}$$

$$\partial\mathcal{A}/\partial\{v_x\} = \partial[\partial v_x]/\partial t = (1+s)[\delta\Re] + (t_k-t_0) \times \left[(1+s)\underline{[\dot{\varepsilon}]}^t + \dot{s}[\delta\Re]\right] = \left[\bar{\partial}v_x\right] \tag{50}$$

$$\partial\mathcal{A}/\partial\{T_x\} = [0] \tag{51}$$

$$\partial\mathcal{A}/\partial\{\varepsilon\} = \partial[\partial\varepsilon]/\partial t = (1+s)\left[\,\underline{v_x}\,\right] + \dot{s}\left[\underline{[x]} + (t_k-t_0)\left[\,\underline{v_x}\,\right]\right] = \left[\bar{\partial}\varepsilon\right] \tag{52}$$

$$\partial\mathcal{A}/\partial s = \partial\{\partial s\}/\partial t = [\partial\Re]\{v_x\} + \underline{[\dot{\varepsilon}]}^t\,[[\{x\} + (t_k-t_0)\{v_x\}]] = \{\bar{\partial}s\} \tag{53}$$

$$\partial\mathcal{A}/\partial\{\dot{T}_x\} = [I] \tag{54}$$

$$\partial\mathcal{A}/\partial\{\partial\dot{\varepsilon}\} = \partial[\partial\dot{\varepsilon}]/\partial t = (1+s)\,[[\underline{[x]} + (t_k-t_0)\,\underline{[v_x]}]] = \left[\bar{\partial}\dot{\varepsilon}\right] \tag{55}$$

$$\partial \mathcal{A}/\partial \dot{s} = \partial\{\partial \dot{s}\}/\partial t = [\delta \Re]\,[\![\{x\} + (t_k - t_0)\{v_x\}]\!] = \{\bar{\partial}\dot{s}\} \tag{56}$$

Thus, the contribution to the Jacobian $[J]$ after taken the partials of Eq. (48) is formed by the matrices:

$$[C_V] = \begin{bmatrix} [\bar{\partial}x] & [0] & \dots & [0] & | & [\bar{\partial}v_x] & [0] & \dots & [0] \\ [0] & [\bar{\partial}x] & \dots & [0] & | & [0] & [\bar{\partial}v_x] & \dots & [0] \\ \cdot & \cdot & & \cdot & | & \cdot & \cdot & & \cdot \\ \cdot & \cdot & \cdot & \cdot & | & \cdot & \cdot & \cdot & \cdot \\ \cdot & \cdot & & \cdot & | & \cdot & \cdot & & \cdot \\ [0] & [0] & \dots & [\bar{\partial}x] & | & [0] & [0] & \dots & [\bar{\partial}v_x] \end{bmatrix}_{(3n\times 6n)} = \underset{3n\times 3n}{[[C_{V1}]} \vdots \underset{3n\times 3n}{[C_{V2}]] } \tag{57}$$

and

$$[D_V] = \begin{bmatrix} [0] & | & [\bar{\partial}\varepsilon]_1 & | & \{\bar{\partial}s\}_1 & | & [I] & | & [\bar{\partial}\dot{\varepsilon}]_1 & | & \{\bar{\partial}\dot{s}\}_1 \\ [0] & | & [\bar{\partial}\varepsilon]_2 & | & \{\bar{\partial}s\}_2 & | & [I] & | & [\bar{\partial}\dot{\varepsilon}]_2 & | & \{\bar{\partial}\dot{s}\}_2 \\ \cdot & | & \cdot & | & \cdot & | & \cdot & | & \cdot & | & \cdot \\ \cdot & | & \cdot & | & \cdot & | & \cdot & | & \cdot & | & \cdot \\ \cdot & | & \cdot & | & \cdot & | & \cdot & | & \cdot & | & \cdot \\ [0] & | & [\bar{\partial}\varepsilon]_n & | & \{\bar{\partial}s\}_n & | & [I] & | & [\bar{\partial}\dot{\varepsilon}]_n & | & \{\bar{\partial}\dot{s}\}_n \end{bmatrix}_{(3n\times 14)} = \underset{3n\times 7}{[[D_{V1}]} \vdots \underset{3n\times 7}{[D_{V2}]] } \tag{58}$$

Fig. 2
Differences between the transformed ITRF97 and published ITRF97 positions

Final variance–covariance matrix

The variance–covariance matrix of the transformed coordinates and velocities on the frame ITRFzz at time t will be computed using Eq. (24), namely

$$\sum\nolimits_{s'} = [J] \sum\nolimits_{s} [J]^t; \tag{59}$$

where the Jacobian $[J]$ is expressed in compact form by:

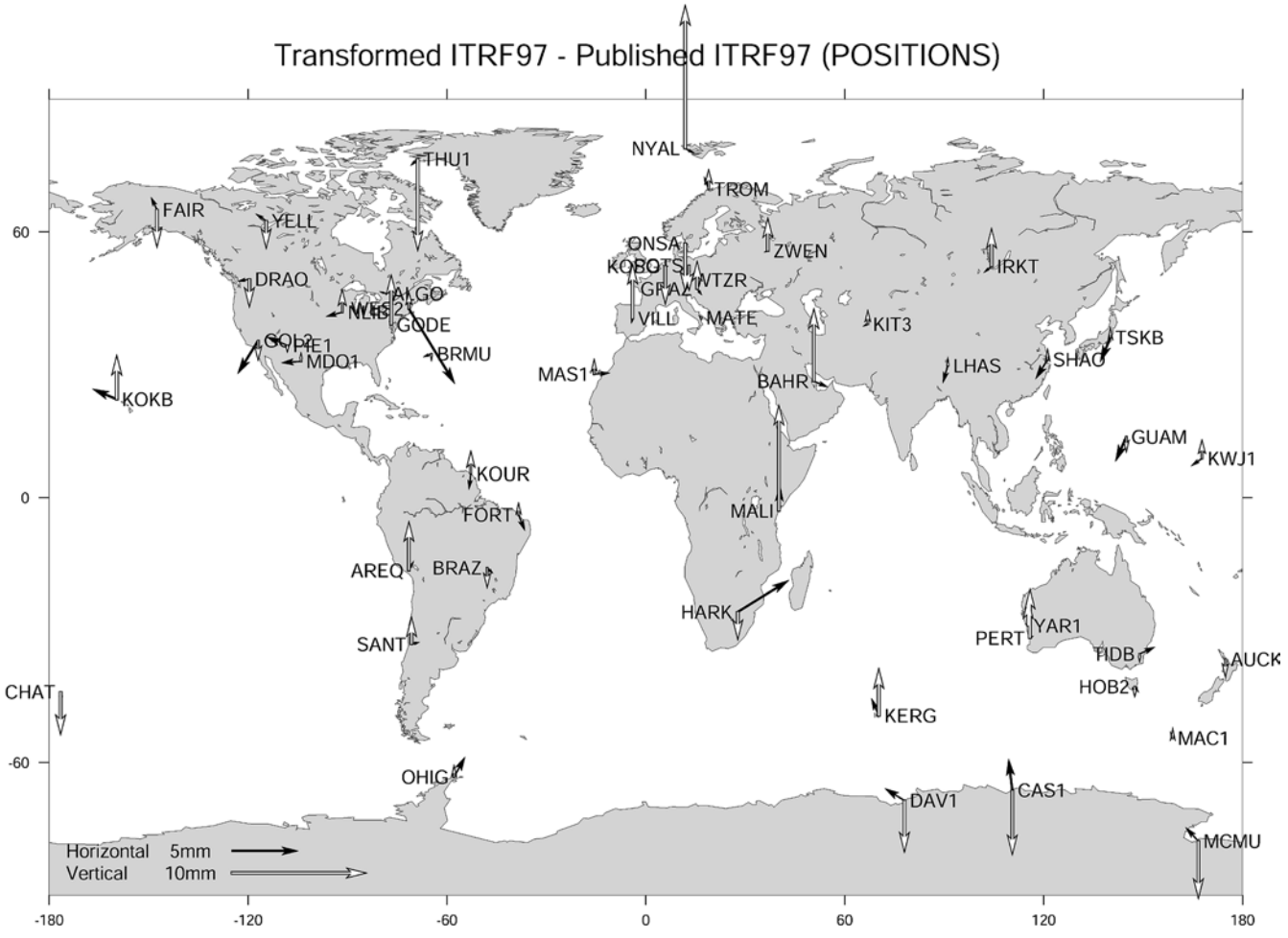

$$[J] = \begin{bmatrix} [C_1]_{(3n\times 3n)} & [C_2]_{(3n\times 3n)} & [D_1]_{(3n\times 7)} & [D_2]_{(3n\times 7)} \\ [C_{V_1}]_{(3n\times 3n)} & [C_{V_2}]_{(3n\times 3n)} & [D_{V_1}]_{(3n\times 7)} & [D_{V_2}]_{(3n\times 7)} \end{bmatrix}_{(6n)\times(6n+14)} \quad (60)$$

It should be mentioned here that the general formulation for propagating variance–covariance matrices of GPS-determined vector components (not coordinates) related through a seven-parameter transformation was already given in (Soler 2001).

Practical example

A practical example is provided here to illustrate the theory just described. We carry out a familiar task in geodesy and surveying where positions and velocities are transformed to a common reference frame and epoch. Specifically, we transform published ITRF00 (1997.0) positions and velocities to ITRF97 (1997.0) using the published 14 transformation parameters and using the expressions developed in this paper. We then compare our transformed ITRF00 (1997.0) values with the published ITRF97 (1997.0) values.

Our case study is based on the standard files used by IGS to archive network solutions. We are referring to the so-called SINEX files (ftp://igs.jpl.nasa.gov/igscb/data/format/sinex.txt). These files were structured to be general and modular enough to handle any type of space geodesy technique including GPS. SINEX files are inter-compatible in the sense that output files can be used, in subsequent analysis, as input files or vice versa, if desired. Another advantage of the format of SINEX files is that the stored a priori information can be removed, thereby permitting users to apply their own corrections (e.g., antenna heights, phase center offsets). SINEX files are ideal for exchanging station coordinates and velocity information and this is the main reason for using them in the present study. Most importantly, each SINEX solution contains the variance–covariance (upper or lower triangular) and full cross-covariances of the positions and velocities [matrix Σ_{CV} in Eq. (25)].

Fig. 3
Differences between the transformed ITRF97 and published ITRF97 velocities

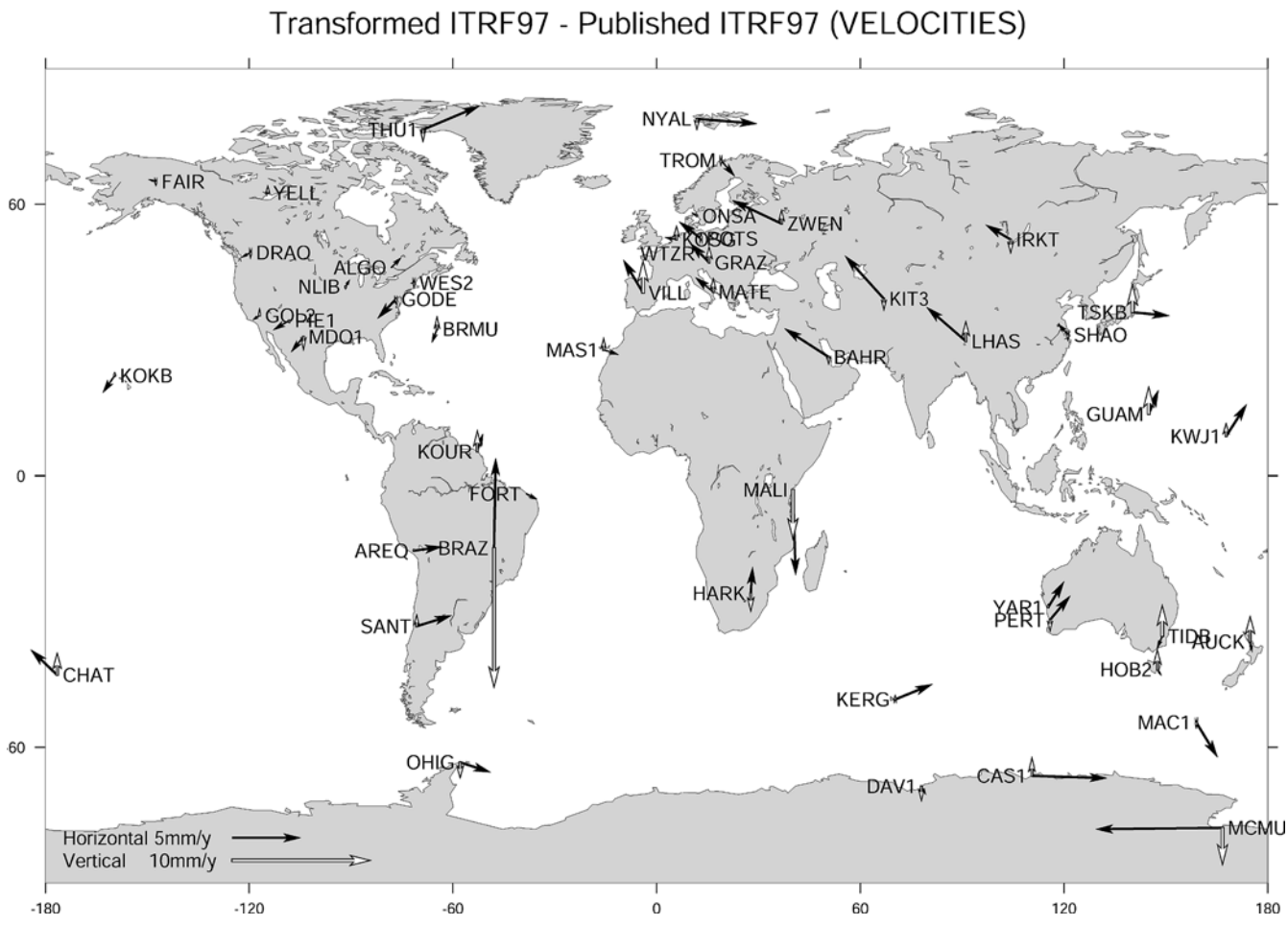

The transformation considered in our example was ITRF00 (epoch 1997.0) → ITRF97 (epoch 1997.0), where the 14-transformation parameters between the two frames (IGS realization) are given at epoch t_k=2001.5 (Ferland 2002). We could have selected a more general case with different epochs for the initial and final frames; however, the SINEX files of the two frames involved are readily available from the IERS data archives at epoch 1997.0. Our main intent was to use the rigorous formulation advanced in this paper to transform the newest frame realization (ITRF00) to a previous one (e.g., ITRF97), analyzing in the process how the transformed ITRF97 results compare with the original published values of ITRF97. The number of stations selected for the transformation was 51, the core of fiducials spanning a subset of high-quality, well-distributed, global station network, the so-called reference frame (RF) stations employed by the analysis centers (AC) to compute IGS combined orbits. First, from the ITRF00 SINEX file (ITRF2000_GPS.SNX.gz) available via anonymous ftp (lareg.ensg.ign.fr in directory pub/itrf/itrf2000), we extracted and reordered the variance–covariance and cross-correlation matrices of the positions and velocities of the 51 stations involved. Knowing the ITRF00 coordinates of the stations, their velocities, their full variance–covariance matrix, and the 14-parameters with associated variances, we used Eqs. (15), (17), and (60), in conjunction with (59), to determine the transformed coordinates, transformed velocities and final transformed and fully populated variance–covariance matrix in the ITRF97 frame. The resulting values were compared with the quantities published in the original ITRF97 SINEX file (ITRF97_GPS.SNX.gz), also available via anonymous ftp at the same web address and directory pub/itrf/itrf97. Differences between our transformed ITRF97 positions and the original IERS published ITRF97 positions (e.g., Boucher et al. 1999) were calculated and plotted. Figure 2 shows the plot of the position differences where the black arrows are the horizontal differences projected on a local topocentric plane at each station, whereas the white arrows are the differences along the vertical component. The figure clearly shows that, in the horizontal case, all differences are smaller than 5 mm, except for station Westford (WES2). It is well known that the Westford site has had chronic position problems and some of the reductions of the local surveys used in the generation of ITRF00 and/or ITRF97 coordinates may not be fully accurate. This could be one of the reasons for the larger than usual horizontal discrepancy found at this station, although the actual cause of the problem is unknown at this time. To close this issue it suffices to invoke the quotation by Altamimi et al. (2000, p. 360): "The peculiar case of the Westford site still

Fig. 4
Horizontal standard error ellipses for the transformed and published ITRF97 positions

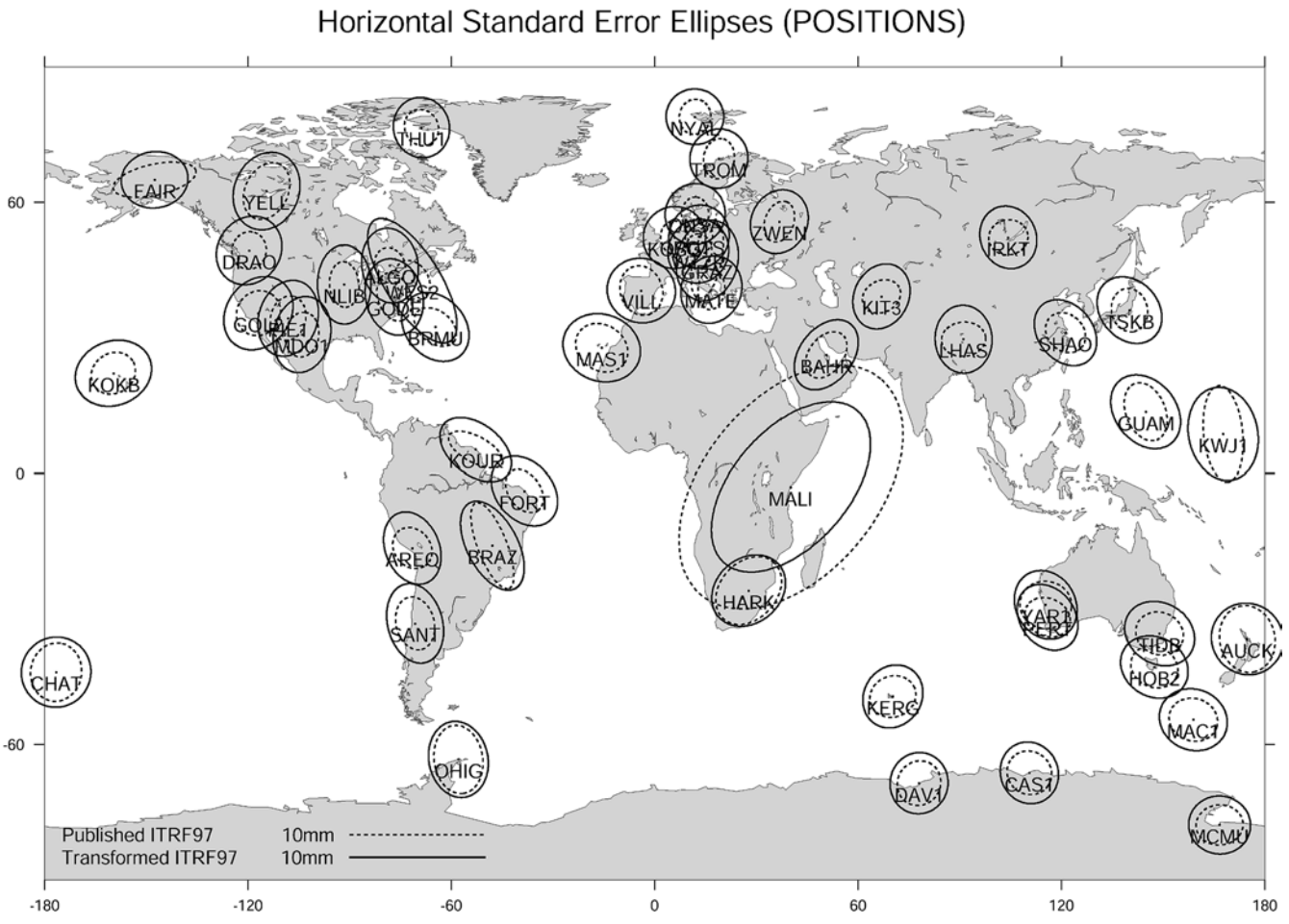

needs attention". Overall, the orientation of the horizontal arrows appears to be random and the results obtained show an apparent improvement over previously published studies comparing transformation residuals between ITRF96 and ITRF97 (Kouba et al. 1998). As expected, station position discrepancies along the vertical component (white arrows) are larger than their horizontal counterparts. Meanwhile, we can state that the vertical differences do not exceed 1 cm except for station NYAL which, although presenting negligible differences on the horizontal component, shows a vertical difference of 10.6 mm. This situation is a recurrent case found before by other investigators (e.g., Kouba et al. 1998).

The differences plotted in Fig. 2, although not significant, could be attributed to a combination of several factors. Probably, the coordinates of the ITRF97 solution are not as accurate as their ITRF00 counterpart, primarily because they were derived using less precise orbits and included a fewer number of years of reliable GPS data. Another possible source for the detected discrepancies could be unknown small errors implicit in the 14-transformation parameters. These parameters have been determined from a set of 49 stations that are not exactly the same as the ones selected for this study. Some stations with large residuals present in our results may have been down-weighted and/or edited out and discarded from the solution generating the transformation parameters; thus, strictly speaking, the network geometry is not identical. Moreover, recall that in the analysis presented here, the variance–covariance matrix of the transformation parameters was assumed diagonal and that cross-covariances between positions, velocities, and transformation parameters were assumed zero because they are not published anywhere. It is expected that, with time, once the long-term behavior of the selected RF stations is established, and when more complete information about the variance–covariance matrix of the transformation parameters becomes available, the discrepancies shown on the plots will be further reduced.

Figure 3 depicts the velocity differences plotted, as before, on the topocentric horizontal and vertical planes. Once more, except at station BRAZ, the results show small differences between the transformed ITRF97 set of velocities and the published ITRF97 values. The discrepancies at station BRAZ more than likely reflect the fact that the velocity components of this station along the vertical on ITRF00 are very different from the velocities published for ITRF97 (0.0015 vs. –0.0088 m/year). The precise determination of the vertical velocity at BRAZ remains a challenge, although it could be conjectured that the latest ITRF00 solution is of better quality than the older ITRF97 results. Figure 3 also shows that after the ITRF00 velocities are

Fig. 5
Horizontal standard error ellipses for the transformed and published ITRF97 velocities

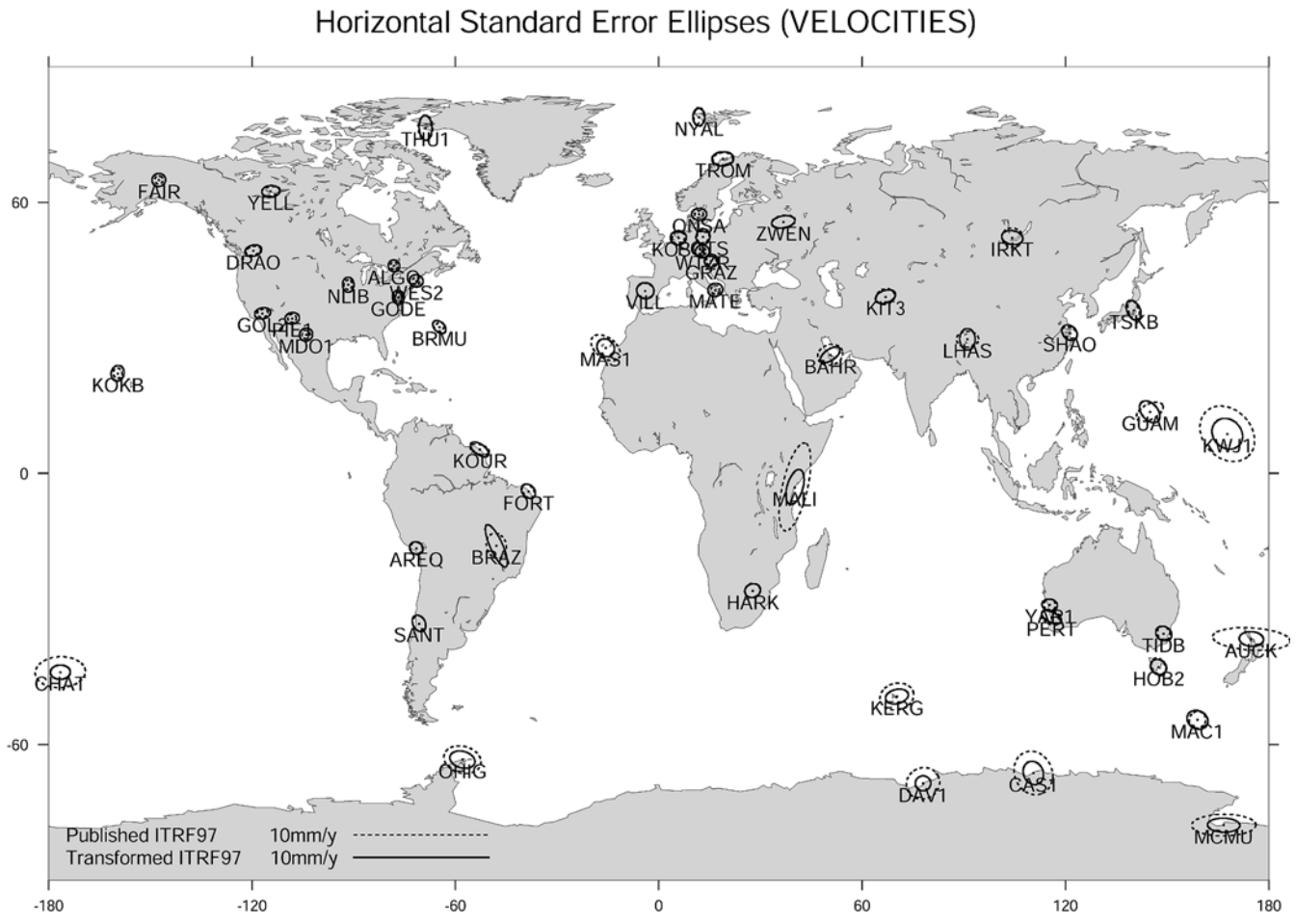

transformed to ITRF97 and differenced with the published ITRF97 values, small residuals caused by the effect of plate rotation are apparent. We suspect that this may indicate that the rotation of the plates was not fully accounted for on the ITRF97 solution. There are three stations, BAHR, KIT3, and LHAS, where some systematic trend, common to the three stations, is clearly evident. These are relatively new stations that started to operate around 1995 and may not have adequate data to determine accurate velocities. For example, the arrow at BAHR in Fig. 3 represents about 10% of the published ITRF97 velocity values (v_e=30.5 mm/y; v_n=28.8 mm/y). On the other hand, the North American sites clearly show the typical rotation of the plate, although the differences obtained are practically negligible, corroborating the overall excellent performance of quality stations that are collecting data for a longer time. Figure 4 presents the standard error ellipses of the transformed ITRF00 variance–covariance matrix at each station compared with the corresponding standard error ellipses obtained from the published ITRF97 SINEX file. In almost every case, the transformed error ellipses are larger than the published ones. This may be caused by the large sigmas associated with the rotation parameters ϵ_x, ϵ_y, ϵ_z. Notice that the parameters $\varepsilon_x, \varepsilon_y, \dot{\varepsilon}_x,$ and $\dot{\varepsilon}_y$ are not statistically significant. In another words, the 1σ values attached to the coordinates of the ITRF97, and perhaps ITRF00, appear to be too optimistic. One exception is station MALI, where we speculate the velocity uncertainties were downgraded in one of the two solutions compared in this particular example.

Figure 5 is equivalent to Fig. 4 except that the plots represent horizontal standard error ellipses for velocities. However, at a few stations, primarily in the southern hemisphere, the pattern of Fig. 4 is reversed. That is, the transformed standard error ellipses are smaller in size than the published ones implying that, perhaps, the new ITRF00 velocities because they are determined from data bases spanning a larger total number of years appear to be closer to true values than the errors published in past solutions. Finally, Figs. 6 and 7 depict the vertical standard error bars for the positions and velocities, respectively. A glance at Fig. 6 indicates that the vertical component at most stations is inside the 1-cm error level. On the other hand, the upper bound for velocities is 2 mm/year. The transformed errors appear to be more realistic than the published over-optimistic formal errors, primarily because now the effects of the uncertainties implicit in the parameters are propagated into the results. Plots such as the ones presented here have the advantage of displaying the relative behavior of every station with respect to all others and, we believe, are more appealing than long tabulations of figures. Therefore, intentionally, all plotted differences and

Fig. 6
Vertical standard error bars for the transformed and published ITRF97 positions

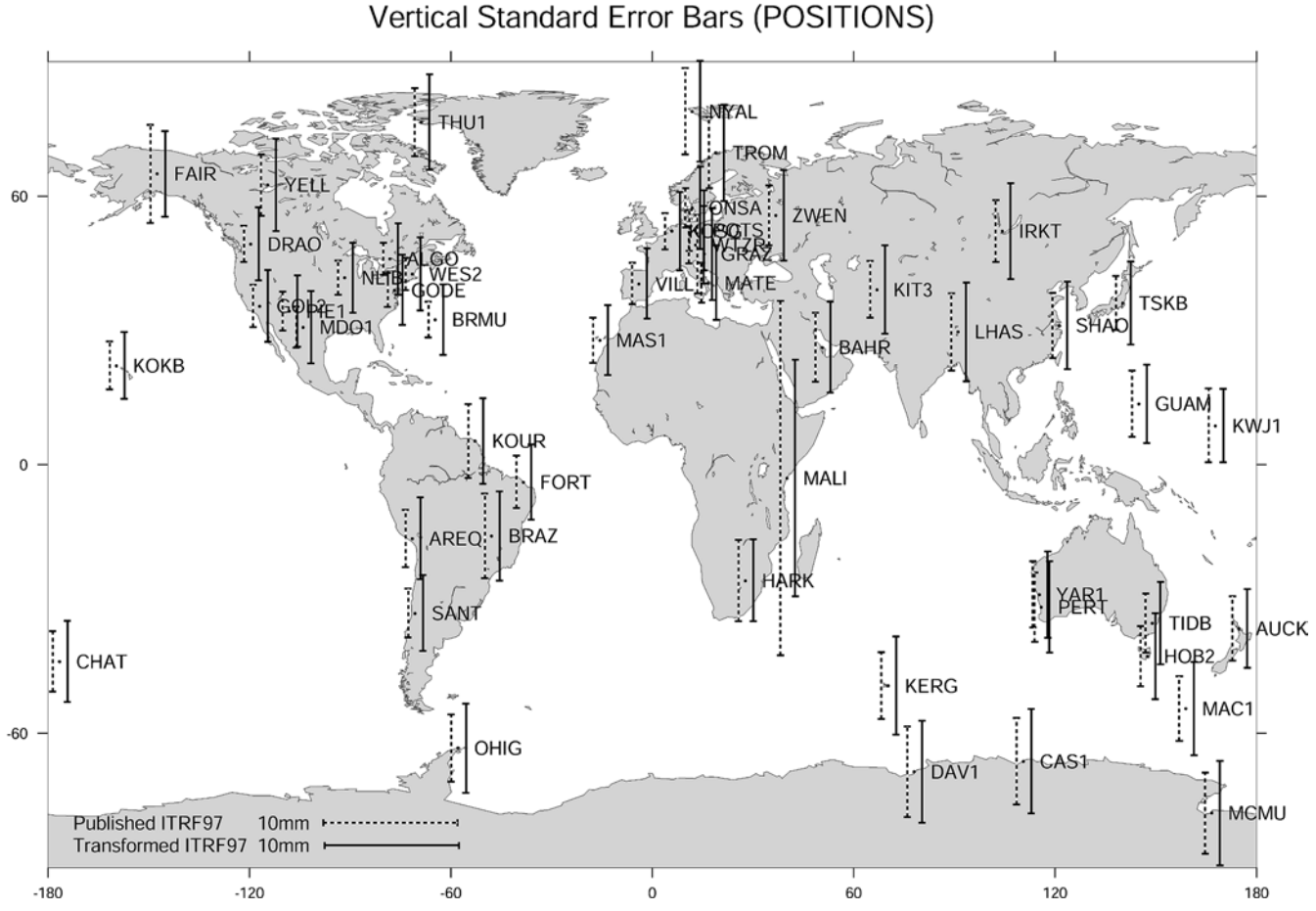

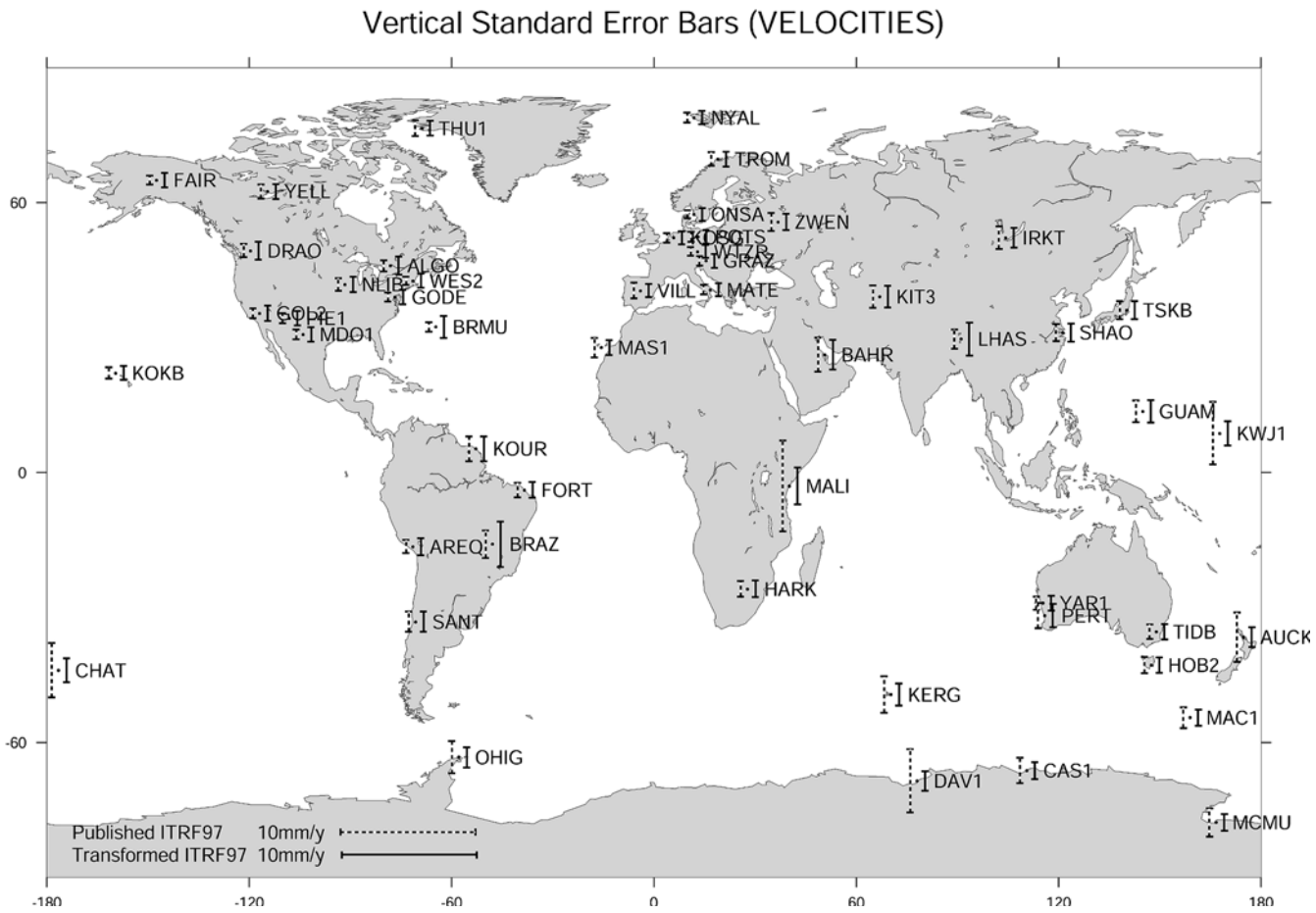

Fig. 7
Vertical standard error bars for the transformed and published ITRF97 velocities

standard errors were drawn at the same scale. Notice that the error bars of Figs. 6 and 7 are highly correlated with their corresponding standard error ellipses. Thus, when we analyze this information in the context of the discussion of Figs. 4 and 5, the graphical interpretation could be extended to larger vs. smaller 3-D error ellipsoids.
The reported results are encouraging. The immediate conclusion is that it may not be necessary to archive old SINEX files from past epochs if we are given a precise variance–covariance matrix for the 14 parameters between reference frames. It probably will be more accurate to keep only the SINEX file of the latest available solution, at the epoch that it was determined, and the set of 14-parameters and variance–covariance matrix of the transformation, at certain epoch t_k, between this solution and any other solution/frame. With these values as input, the positions, velocities, and variance–covariance matrix at any other epoch could be obtained using the formulation introduced in this paper.

Conclusions

The growing number of global, continental, national, and regional GPS networks often requires the rigorous transformation of station coordinates and velocities between different frames and epochs. Not only the coordinates of the points and their velocities should be transformed using the most recent values of the seven parameters and their rates, but the variance–covariance matrix of these coordinates and velocities should also be propagated taking into consideration all available stochastic information. This paper introduces new rigorous matrix equations to update the variance–covariance matrix involved in 14-parameter similarity transformations. It is the only way to obtain a unified and consistent set of station position and velocities with appropriate variance–covariance matrices necessary for any regional combination of coordinates from previous solutions at some specific epoch. This procedure could avoid the re-processing of the original GPS observations, an arduous task sometimes difficult to implement.
Furthermore, the geodetic community, spearheaded by the IGS, is starting to use SINEX files as standard input/output format for all types of GPS data analysis. These files contain the Cartesian coordinates and velocities of the points involved in any particular solution at a pre-specified epoch, say t_0. Additionally, the SINEX files also provide the full variance–covariance matrix of the coordinates and velocities; consequently, matrices Σ_C, Σ_V, and Σ_{CV} in Eq. (25) are known. Similarly, the diagonal elements of matrices Σ_P and $\Sigma_{\dot{P}}$ and their cross-covariance $\Sigma_{P\dot{P}}$ at epoch t_k are provided by international organizations

(IERS, IGS) through periodical tabulations published whenever a new ITRF frame is adopted. It is recommended that, in order to achieve more accurate results, the full variance–covariance matrices Σ_P and $\Sigma_{\dot{P}}$ and their cross-correlation should be distributed to the public. In conclusion, applying the theory introduced here, it is feasible to rigorously determine the transformed coordinates and velocities and their full variance–covariance matrix between any two frames $ITRF_{yy}(t_0) \rightarrow ITRF_{zz}(t)$ using as input the stochastic model of the coordinates and velocities and the 14 parameters involved in the transformation. In essence, the result of our analysis suggest that from the most recent SINEX file at certain epoch t_0 and the 14-transformation parameters at epoch t_k, the positions, velocities, and full variance–covariance of SINEX files at any arbitrary epoch t could be conveniently determined.

Acknowledgements The authors greatly appreciate the help of B.H.W. van Gelder, S.A. Hilla, D.G. Milbert, C.R. Schwarz, and J.M. Young whose comments significantly improved the contents and readability of the manuscript. Several figures were generated with the Generic Mapping Tools software (Wessel and Smith 1991).

References

Altamimi Z, Boucher C, Sillard P (2000) ITRF97 and quality analysis of IGS reference stations. 1999 technical report. International GPS Service for Geodynamics, Pasadena, pp 353–360

Argus DF, Gordon RG (1991) No-net-rotation model of current plate velocities incorporating plate rotation model NUVEL-1. Geophys Res Lett 18:2039–2042

Boucher C, Altamimi Z, Sillard P (1999) The international reference frame (ITRF97). IERS technical note 27. Central Bureau of IERS, Observatoires de Paris, Paris

DeMets C, Gordon RG, Argus DF, Stein S (1994) Effect of recent revisions to the geomagnetic reversal time scale on estimates of current plate motions. Geophys Res Lett 21:2191–2194

Ferland R (2002) IGS reference frame coordination and working group activities. 2001 IGS Annual Report, Jet Propulsion Lab, Pasadena, pp 24–27

Kaula WM (1966) Theory of satellite geodesy. Blaisdell Publishing, Waltham, MA

Kouba J, Ray J, Walkins MM (1998) IGS reference frame realization. Proceedings 1998 Analysis Center Workshop, Darmstadt, Germany, 9–11 February, pp 139–171

McCarthy D (ed) (1996) IERS technical note 21. Observatoire de Paris, Paris

Moore AW (2002). The growth of the IGS network. 2000 Annual Report. International GPS Service for Geodynamics, Jet Propulsion Lab, Pasadena, pp 11–13

Mueller II (1969) Spherical and practical astronomy as applied to geodesy. Ungar, New York

Snay RA, Weston ND (1999) Future directions of the National CORS system. Proc 55th Annual meeting of the Institute of Navigation, 28–30 June, Cambridge, MA. Alexandria, VA, pp 301–305

Soler T (1998) A compendium of transformation formulas useful in GPS work. J Geodesy 72:482–490

Soler T (2001) Densifying 3D networks by accurate transformation of GPS-determined vector components. GPS Solutions 4:27–33.

Springer TA, Hugentobler U (2001) IGS ultra rapid products for (near-) real-time applications. Phys Chem Earth 26:623–628

Wessel P, Smith WHF (1991) Free software helps map and display data. EOS Trans Am Geophys Union 72:26